

Pauli Propagation for Imaginary Time Evolution

Rafael Gómez-Lurbe¹ and Armando Pérez¹

¹Departament de Física Teòrica and IFIC, Universitat de València-CSIC, 46100 Burjassot (València), Spain*

We extend the Pauli Propagation framework to simulate imaginary time evolution. By deriving explicit update rules for the propagation of Pauli operators under imaginary time evolution generated by Pauli strings, we introduce an imaginary time Pauli Propagation (ITPP) algorithm for approximating imaginary time dynamics directly in the Pauli basis. This approach enables the computation of thermal and ground-state properties while retaining the key computational advantages of Pauli Propagation. Benchmarking ITPP on the one-dimensional transverse-field Ising model demonstrates that truncation provides a controlled trade-off between accuracy and computational cost, while also revealing challenges associated with operator growth under imaginary time evolution. Finally, combining imaginary time and real-time Pauli Propagation naturally suggests a pathway toward simulating open quantum system dynamics within a unified framework.

I. INTRODUCTION

Classical simulation of quantum many-body systems is notoriously challenging due to the exponential growth of the Hilbert-space dimension with system size, rendering exact diagonalization rapidly intractable. As a consequence, approximate numerical methods are indispensable. Established techniques such as tensor network algorithms [1, 2] and quantum Monte Carlo [3, 4] have enabled substantial progress, yet they also face well-known limitations, including entanglement growth in out-of-equilibrium dynamics [5, 6] and sign-problem constraints in frustrated or fermionic models [7, 8].

A recently introduced approach for approximately simulating quantum dynamics is *Pauli Propagation* [9, 10], also known as *sparse Pauli dynamics* [11]. In contrast to conventional Schrödinger-picture simulations that evolve a quantum state, Pauli Propagation works in the Heisenberg picture by expanding observables in the Pauli operator basis and evolving their coefficients in time. Operator growth is controlled by truncating the Pauli expansion and retaining only the most significant terms. This strategy is computationally attractive because Pauli operators admit efficient bitstring representations and their multiplication and commutation relations reduce to simple bitwise operations. Using this framework, state-of-the-art classical simulations of real-time quench dynamics in two- and three-dimensional transverse-field Ising models have been demonstrated [12]. Furthermore, Ref. [13] shows that Pauli Propagation can also be used to classically estimate expectation values of arbitrary observables on random unstructured quantum circuits.

The original formulation of Pauli Propagation applies to real-time dynamics. In this work, we extend Pauli Propagation to imaginary time evolution. *Imaginary time evolution* (ITE) is a fundamental tool for state preparation, enabling access to thermal states and filtering toward ground states, and is routinely implemented in classical simulation methods such as quantum Monte

Carlo [3] and tensor-network algorithms [1]. We derive explicit rules governing the evolution of Pauli operators under imaginary time evolution generated by arbitrary Pauli strings. Building on these rules, we construct an algorithm for approximating thermal and ground-state observables. As in real-time Pauli Propagation, the number of Pauli terms typically grows rapidly under imaginary time evolution, requiring truncation strategies to retain computational feasibility. Moreover, the ability to handle non-unitary imaginary time evolution within the Pauli Propagation framework opens the door to combining imaginary- and real-time dynamics, thus enabling the simulation of open quantum system dynamics [14].

To benchmark the method and to assess its practical performance, we apply the imaginary time evolution Pauli Propagation algorithm (ITPP) to the one-dimensional transverse-field Ising model in the ordered phase. We compare its results with Trotterized imaginary time evolution and exact calculations, and we examine several truncation strategies, including coefficient thresholds and fixed-rank schemes.

The paper is organized as follows. In Sec. II, we briefly review imaginary time evolution, thermal states, and the standard Pauli Propagation algorithm for real-time dynamics. Next, we introduce our extension of Pauli Propagation to imaginary time dynamics. Numerical experiments are presented in Sec. III. Finally, Sec. IV summarizes our findings and discusses possible future directions.

II. THEORY

In this section, we review the theoretical background underlying our approach. We begin by summarizing imaginary time evolution and its connection to thermal and ground states. We then outline the standard Pauli Propagation algorithm for real-time dynamics. Finally, we introduce our extension of Pauli Propagation to imaginary time evolution, which forms the basis of the method used in this work.

* rafael.gomez-lurbe@uv.es

A. Imaginary Time Evolution

Imaginary time evolution provides a powerful framework for accessing thermal and ground-state properties of quantum many-body systems. Starting from a pure quantum state $|\psi_0\rangle$, imaginary time evolution is defined through the non-unitary transformation

$$|\psi(\tau)\rangle = \frac{e^{-\tau\hat{H}}|\psi_0\rangle}{\sqrt{\langle\psi_0|e^{-2\tau\hat{H}}|\psi_0\rangle}}, \quad (1)$$

where $\tau \geq 0$ plays the role of an *imaginary time*. The normalization in the denominator is required to obtain a valid quantum state because $e^{-\tau\hat{H}}$ is not unitary. Provided that the initial state $|\psi_0\rangle$ has nonzero overlap with the ground state of \hat{H} , the evolved state $|\psi(\tau)\rangle$ converges to the ground state as $\tau \rightarrow \infty$.

More generally, imaginary time evolution can be formulated at the level of density matrices. Given an initial density matrix ρ_0 , its imaginary time evolved state is defined as

$$\rho(\tau) = \frac{e^{-\tau\hat{H}}\rho_0e^{-\tau\hat{H}}}{\text{Tr}[e^{-2\tau\hat{H}}\rho_0]}. \quad (2)$$

This expression ensures proper normalization, $\text{Tr}[\rho(\tau)] = 1$, at all imaginary times.

In the limit $\tau \rightarrow \infty$, and provided that ρ_0 has a nonzero overlap with the ground-state subspace, the density matrix $\rho(\tau)$ converges to the ground-state projector,

$$\rho(\tau) \xrightarrow{\tau \rightarrow \infty} |\psi_{\text{gs}}\rangle\langle\psi_{\text{gs}}|, \quad (3)$$

where $|\psi_{\text{gs}}\rangle$ denotes the ground state of \hat{H} .

A particularly important case is obtained by choosing the initial state to be the maximally mixed state,

$$\rho_0 = \frac{1}{2^n} \mathbb{I},$$

where n denotes the number of spins in the system.

In this case, the imaginary time evolution defined in Eq. (2) yields, for an arbitrary imaginary time 2τ , the thermal state

$$\rho_{\text{th}}(\tau) = \frac{e^{-2\tau\hat{H}}}{\text{Tr}[e^{-2\tau\hat{H}}]}, \quad (4)$$

obtained by evolving the infinite-temperature state at $\tau = 0$ to imaginary time 2τ , which sets the inverse temperature. In the zero-temperature limit, $\tau \rightarrow \infty$, the imaginary time evolution converges to a projector onto the ground state.

Expectation values of observables \hat{O} at imaginary time 2τ are obtained as

$$\langle\hat{O}\rangle_{\tau} = \text{Tr}[\hat{O}\rho(\tau)] = \frac{\text{Tr}[\hat{O}e^{-\tau\hat{H}}]}{\text{Tr}[e^{-\tau\hat{H}}]}. \quad (5)$$

In the zero-temperature limit $\tau \rightarrow \infty$, the thermal state $\rho(\tau)$ projects onto the ground state of \hat{H} , and the expectation value $\langle\hat{O}\rangle_{\tau}$ reduces to the ground-state expectation value of \hat{O} .

Several classical approaches have been developed to approximate imaginary time evolution, most notably quantum Monte Carlo [3] and tensor-network algorithms [1]. In recent years, quantum algorithms for approximating imaginary time evolution on quantum hardware have also been proposed. Approaches such as Quantum Imaginary Time Evolution (QITE) [15] and its variational variant (VQITE) [16] implement imaginary time evolution directly on a quantum computer in the Schrödinger picture. For a pedagogical introduction to these methods, see Ref. [17].

B. Pauli Propagation

Pauli Propagation is a classical algorithm for simulating quantum dynamics by evolving observables in the Heisenberg picture, rather than state vectors. In this framework, an observable O evolves as

$$O(t) = U^{\dagger}(t)O U(t), \quad (6)$$

with $U(t) = \exp(-itH)$, where H is the system Hamiltonian.

The key idea is to expand the observable in the Pauli basis:

$$O = \sum_{P \in \mathcal{P}} c_P P, \quad (7)$$

where \mathcal{P} is a set of Pauli operators and c_P are real coefficients. The evolution of a Pauli operator P under a Pauli rotation $U_Q(\theta) = \exp(-iQ\theta/2) = \cos(\frac{\theta}{2})\mathbb{I} - i\sin(\frac{\theta}{2})Q$ satisfies

$$U_Q(\theta)^{\dagger} P U_Q(\theta) = \begin{cases} P, & [P, Q] = 0, \\ \cos(\theta)P + i\sin(\theta)QP, & \{P, Q\} = 0, \end{cases} \quad (8)$$

where $[\cdot, \cdot]$ and $\{\cdot, \cdot\}$ denote the commutator and anticommutator, respectively. This identity enables each term in the Pauli decomposition of Eq. 7 to be propagated independently.

For a Hamiltonian decomposed as $H = \sum_j \alpha_j h_j$ with Pauli operators h_j , the exact evolution operator can be approximated via a first-order Trotter expansion:

$$U(t) = \left(\prod_j \exp(-i\alpha_j \Delta t h_j) \right)^n + \mathcal{O}(\Delta t), \quad (9)$$

where $n = t/\Delta t$. This expresses $U(t)$ as a sequence of single-Pauli rotations, each applied iteratively to propagate the observable.

A challenge of Pauli Propagation is the exponential growth of terms in $O(t)$, as each rotation can generate new Pauli strings. To maintain the computational cost tractable, truncation strategies are employed:

- **Coefficient threshold:** retain only Pauli terms with coefficients satisfying $|c_P| > \delta$, where δ is a chosen threshold parameter.
- **Pauli weight cutoff:** retain terms whose Pauli weight (number of non-identity operators) does not exceed a fixed threshold.

Coefficient-based truncation is practical and widely used [12], while weight-based truncation allows rigorous bounds on computational cost and approximation error [13]. Each method balances efficiency and accuracy differently, depending on the system and observable structure.

C. Imaginary Time Evolution via Pauli Propagation

Following a similar approach to real-time Pauli Propagation, we define a set of rules to evolve a Pauli operator under an imaginary time Pauli operator

$$V_Q(\tau) = \exp\left(-\frac{\tau}{2}Q\right) = \cosh\left(\frac{\tau}{2}\right)\mathbb{I} - \sinh\left(\frac{\tau}{2}\right)Q, \quad (10)$$

where Q is a Pauli string.

The evolution of a Pauli operator P under this imaginary time operator satisfies

$$V_Q(\tau)^\dagger P V_Q(\tau) = \begin{cases} P, & \{P, Q\} = 0, \\ \cosh(\tau)P - \sinh(\tau)QP, & [P, Q] = 0. \end{cases} \quad (11)$$

where $[\cdot, \cdot]$ and $\{\cdot, \cdot\}$ denote the commutator and anticommutator, respectively. The derivation of these propagation rules is provided in Appendix A.

Interestingly, the propagation rules for a Pauli string under imaginary time evolution are essentially the opposite of those encountered in real-time Pauli Propagation. In particular, when the propagated Pauli string anticommutes with the generator of the imaginary time operator, the operator remains unchanged. By contrast, when the two operators commute, the Pauli string splits into two terms.

This behavior contrasts with the real-time case, where nontrivial evolution arises from anticommuting generators and the resulting coefficients are trigonometric functions reflecting unitarity and norm preservation. In imaginary time evolution, the coefficients are instead hyperbolic functions, corresponding to the non-unitary nature of the dynamics.

Together, these rules provide a natural extension of Pauli Propagation to imaginary time evolution, enabling

the simulation of non-unitary dynamics and the estimation of thermal and ground-state properties within the Pauli operator framework.

Similar to real-time evolution, consider a Hamiltonian decomposed as $\hat{H} = \sum_j \alpha_j h_j$, where h_j are Pauli operators. The exact imaginary time evolution operator,

$$V(\tau) = e^{-\tau\hat{H}}, \quad (12)$$

can be approximated using a first-order Trotter expansion. Writing $\tau = n\Delta\tau$, we define the Trotterized evolution operator

$$V_{\text{Trotter}}(\tau) = \left(\prod_j \exp(-\alpha_j \Delta\tau h_j) \right)^n. \quad (13)$$

The exact evolution is then approximated as

$$V(\tau) = V_{\text{Trotter}}(\tau) + \mathcal{O}(\Delta\tau). \quad (14)$$

This decomposition expresses the imaginary time propagator as a sequence of single-Pauli imaginary time operators, each applied iteratively to propagate a Pauli operator. Combined with the propagation rules described above, this approximation enables the implementation of imaginary time evolution within the Pauli propagation framework. In particular, the thermal state of Eq. (4) can be approximated by propagating the maximally mixed state $\frac{1}{2^n}\mathbb{I}$ through the Trotterized imaginary time propagator, implemented as a sequence of symmetric half-step imaginary time evolutions generated by the individual Pauli terms of the Hamiltonian, with proper normalization. Applying Pauli Propagation in this setting and normalizing by the trace of the resulting operator yields an approximate thermal state

$$\tilde{\rho}_{\text{th}}(\tau) = \frac{\text{PP}\left[V_{\text{Trotter}}\left(\frac{\tau}{2}\right) \hat{I} V_{\text{Trotter}}\left(\frac{\tau}{2}\right)\right]}{\text{Tr}\left(\text{PP}\left[V_{\text{Trotter}}\left(\frac{\tau}{2}\right) \hat{I} V_{\text{Trotter}}\left(\frac{\tau}{2}\right)\right]\right)}. \quad (15)$$

Here, $V_{\text{Trotter}}\left(\frac{\tau}{2}\right)$ denotes the Trotter approximation defined in Eq. (14), and $\text{PP}[\cdot]$ denotes the operator obtained after propagation and truncation in the Pauli basis. To control computational cost, a truncation scheme is applied during propagation, analogous to that employed in Pauli Propagation for real-time dynamics. In practice, the operator is normalized at each propagation step to ensure numerical stability and prevent uncontrolled growth of the Pauli coefficients.

Once the approximate state $\tilde{\rho}_{\text{th}}(\tau)$ is obtained, expectation values of observables \hat{O} can be computed directly as

$$\langle \hat{O} \rangle_\tau \approx \text{Tr}\left[\hat{O} \tilde{\rho}_{\text{th}}(\tau)\right]. \quad (16)$$

This procedure enables the prediction of thermal or ground-state properties while retaining the flexibility to evaluate multiple observables using the same propagated

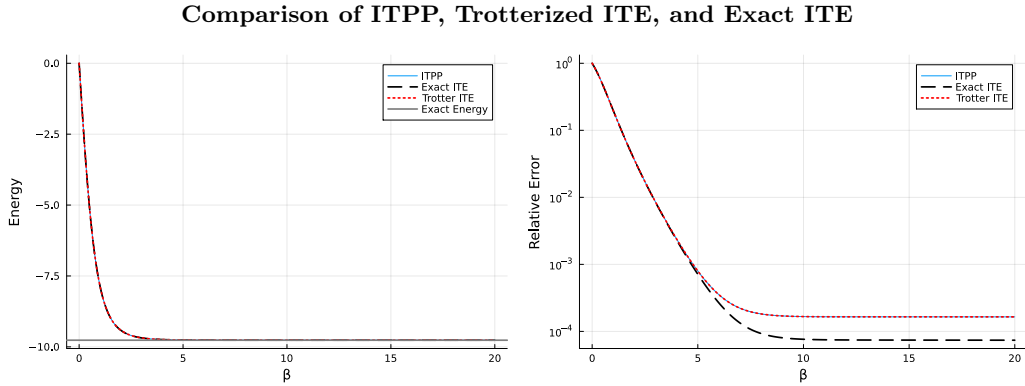


FIG. 1. Comparison of Pauli Propagation imaginary time evolution (ITPP) with Trotterized imaginary time evolution and exact imaginary time evolution for the one-dimensional transverse-field Ising model (TFIM) with $N = 10$ spins, $J = 1$, and $h = 0.5$, using a Trotter step size $\Delta t = 0.04$. The left panel shows the evolution of the energy as a function of imaginary time, while the right panel displays the corresponding relative error with respect to the exact imaginary time evolution, shown on a logarithmic scale. The comparison illustrates the accuracy of ITPP relative to standard Trotterized evolution and the exact result over the course of imaginary time propagation.

operator. By adjusting the truncation threshold and the Trotter step size, one can systematically tune the tradeoff between computational cost and accuracy, making this approach well suited for controlled and flexible studies of quantum many-body systems.

It is important to note that truncation in the Pauli basis does not, in general, preserve positive semidefiniteness. Consequently, the approximate operator $\tilde{\rho}_{th}(\tau)$ may develop negative eigenvalues and therefore fail to represent a valid quantum state, rendering expectation values physically inconsistent. A straightforward way to restore positive semidefiniteness is to square the approximate density operator. This guarantees a positive semidefinite operator but comes at a significant computational cost, as squaring substantially increases the Pauli support. The resulting operator must then be normalized by its trace to recover a properly normalized quantum state. Since the procedure effectively applies the imaginary time evolution twice, the squared operator corresponds to an approximate thermal state at inverse temperature 2τ .

The computational overhead associated with explicitly enforcing positive semidefiniteness can be mitigated using the following identity. Here, $\langle \hat{O} \rangle_{2\tau}$ denotes the expectation value of the observable \hat{O} at imaginary time 2τ , and $\tilde{\rho}_{th}(\tau)$ is the ITPP approximation to the thermal state at imaginary time τ :

$$\langle \hat{O} \rangle_{2\tau} \approx \frac{\text{Tr}[\hat{O} \tilde{\rho}_{th}^2(\tau)]}{\text{Tr}[\tilde{\rho}_{th}^2(\tau)]} = \frac{\text{Tr}[(\hat{O} \tilde{\rho}_{th}(\tau)) \tilde{\rho}_{th}(\tau)]}{\text{Tr}[\tilde{\rho}_{th}^2(\tau)]}. \quad (17)$$

Rather than explicitly constructing $\tilde{\rho}_{th}^2(\tau)$, one can instead compute the Pauli expansion of the product $\hat{O} \tilde{\rho}_{th}(\tau)$ —which typically contains significantly fewer terms—and subsequently evaluate its overlap with $\tilde{\rho}_{th}(\tau)$. The denominator corresponds to the purity of the approximate state and can be computed efficiently

from the L_2 norm of the vector in the Pauli basis. This procedure yields physically meaningful approximations to the expectation values of the observables of interest.

When evolved for sufficiently long imaginary time, this framework enables the extraction of ground-state properties of observables of interest.

III. NUMERICAL EXPERIMENTS

In this section, we present numerical results illustrating the performance of ITPP for approximating ground-state properties of the one-dimensional transverse-field Ising model (TFIM) with open boundary conditions. The Hamiltonian is

$$\hat{H}_{\text{TFIM}} = -J \sum_{i=1}^{n-1} Z_i Z_{i+1} - h \sum_{i=1}^n X_i, \quad (18)$$

where J denotes the nearest-neighbor coupling and h the transverse-field strength. As a reference, we benchmark the ground-state energies obtained from ITPP against exact results computed using the Bogoliubov–de Gennes (BdG) free-fermion solution for the TFIM with open boundaries [18].

All simulations were performed using the `PauliPropagation.jl` Julia package [19], which provides an efficient implementation of Pauli propagation for real-time dynamics. We extend this framework by incorporating the imaginary time propagation rules introduced in Sec. II C.

Since the ordered phase ($J > h$) is known to be the more challenging regime for approximate classical methods, our numerical study focuses on the parameter choice $J = 1.0$ and $h = 0.5$. In this setting, we propagate the identity operator in imaginary time—following the prescription of Sec. II C—and evaluate the converged ground-state energy under various truncation schemes.

ITPP performance for $N = 12$ in the ordered phase ($J = 1, h = 0.5$)

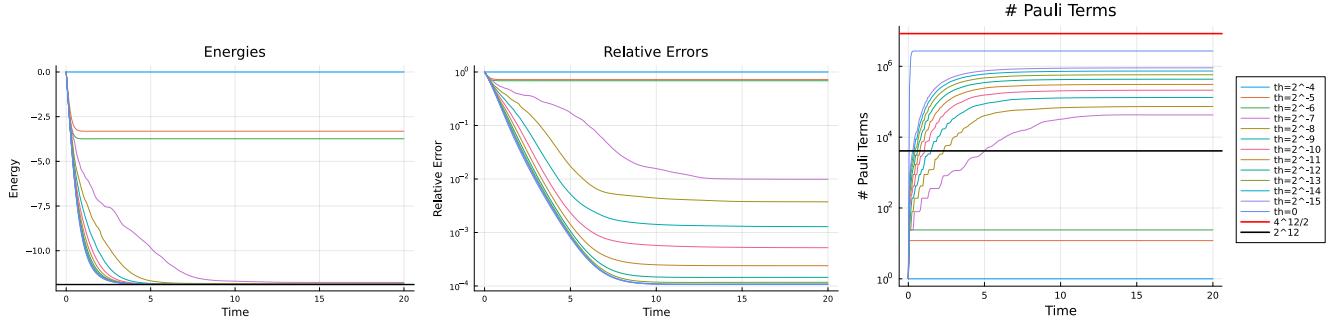


FIG. 2. Performance of ITPP with coefficient-threshold truncation for various thresholds in the ordered-phase TFIM ($J = 1, h = 0.5$) with $N = 12$ spins and Trotter step $\Delta t = 0.04$. The three panels show, from left to right, the energy during imaginary time evolution, the relative error with respect to the exact ground-state energy (displayed on a logarithmic scale), and the number of Pauli terms retained under different truncation thresholds. In the left-most panel, the solid black line indicates the exact ground-state energy computed using the Bogoliubov–de Gennes solution. The results illustrate the trade-off between accuracy and computational cost controlled by the truncation threshold.

We first verify that ITPP faithfully reproduces Trotterized imaginary time evolution and compare its performance against exact imaginary time evolution obtained via exact diagonalization. Simulations are carried out for a chain of $N = 10$ spins and a Trotter step size $\Delta t = 0.04$. Throughout the imaginary time evolution, we track the expectation value of the energy and the relative error with respect to the exact ground-state energy. The corresponding results are presented in Fig. 1.

From the results, we observe that ITPP exactly matches the Trotterized imaginary time evolution, as expected, and closely follows the exact imaginary time evolution until Trotter errors become significant.

We next assess the performance of ITPP under a truncation strategy based on the magnitude of Pauli coefficients. The algorithm is executed using truncation thresholds ranging from 2^{-14} to 2^{-5} , along with the idealized case in which no truncation is applied. Simulations are carried out in the ordered phase of the transverse-field Ising model with parameters $J = 1.0$ and $h = 0.5$, for a chain of $N = 12$ spins and a Trotter step size $\Delta t = 0.04$. Throughout the imaginary time evolution, we track the instantaneous energy, the relative error with respect to the exact ground-state energy, and the number of Pauli terms retained by the algorithm. The corresponding results are presented in Fig. 2.

The numerical results exhibit the expected behavior of ITPP under coefficient-based truncation. As the truncation threshold is decreased, an increasing number of Pauli terms is retained throughout the evolution, leading to progressively more accurate estimates of the ground-state energy. This trend closely parallels what has been observed previously for real-time Pauli Propagation.

A key question is how many Pauli terms are required to obtain a reliable approximation of the ground-state energy. From Fig. 2, we observe that noticeable improvements in accuracy emerge for thresholds below approximately 2^{-7} . In particular, for a threshold of 2^{-7} ,

ITPP attains a relative error of approximately 10^{-2} with respect to the exact ground-state energy while retaining 42,466 Pauli terms. This constitutes a substantial reduction compared to the untruncated ITPP evolution ($\delta = 0$), which involves 2,704,156 Pauli terms.

Across the range of thresholds between 2^{-14} and 2^{-7} , we observe a smooth trade-off between accuracy and computational cost. Lowering the threshold increases the number of retained Pauli terms and improves accuracy at the expense of computational efficiency, whereas increasing the threshold reduces the operator support and computational cost but leads to less accurate energy estimates. Overall, these results demonstrate that ITPP provides a practical framework for estimating ground-state observables, with the truncation threshold offering a systematic means to control the balance between accuracy and efficiency.

For thresholds larger than 2^{-7} , however, we observe a drastic reduction in the number of Pauli terms retained during the evolution, which results in poor approximations of the true ground state. This behavior can be attributed to the tree-like structure underlying Pauli Propagation: during imaginary time evolution, Pauli strings can generate many descendants at later times. If certain branches of this propagation tree are truncated too early, the algorithm discards Pauli terms that would otherwise contribute significantly at later stages. As a result, the evolution becomes confined to an overly restricted operator basis, leading to a loss of accuracy in the final ground-state approximation.

Truncation based on coefficient magnitude provides a natural way to discard Pauli terms by retaining only those with sufficiently large weights. However, this strategy does not offer direct control over the computational cost: fixing a threshold *a priori* does not determine how many Pauli terms will be retained during the evolution. In practice, the number of surviving terms can vary significantly depending on the system size and the stage of

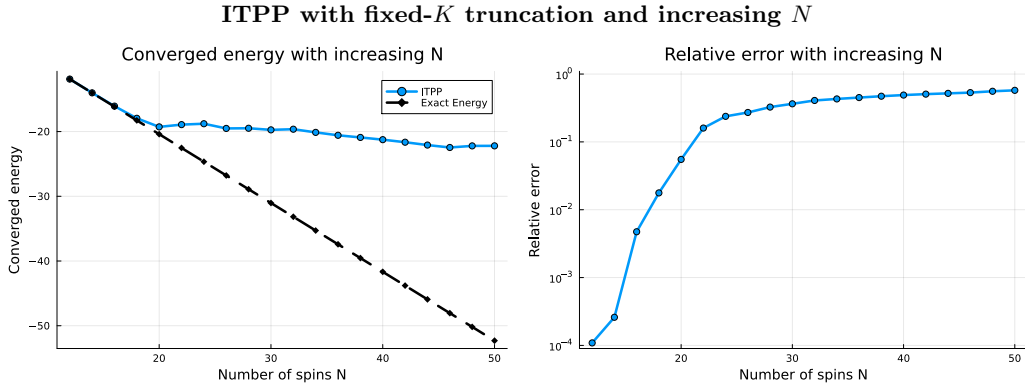


FIG. 3. Scalability of imaginary time Pauli Propagation with fixed- K truncation in the ordered phase of the one-dimensional TFIM ($J = 1$, $h = 0.5$). The left panel shows the converged ground-state energy obtained with ITPP as a function of system size N , while the right panel displays the corresponding relative error (on a logarithmic scale) with respect to the exact ground-state energy computed using the Bogoliubov-de Gennes solution. The truncation parameter is fixed to $K = 2,704,156$, equal to the number of Pauli terms generated for $N = 12$ in the absence of truncation. The results indicate the range of system sizes for which this fixed Pauli basis size is sufficient to accurately capture the underlying operator growth under imaginary time evolution, as well as the onset of a breakdown when the fixed computational budget becomes inadequate.

imaginary time evolution.

Motivated by this limitation and by the need to assess the scalability of the algorithm, we introduce an alternative truncation strategy based on retaining a fixed number of Pauli terms. In this approach, we impose a maximum Pauli basis size K . Whenever the number of Pauli terms exceeds K , all terms are sorted according to the magnitude of their coefficients, and only the K largest contributions are retained. In the case of equal-magnitude coefficients, ties are resolved by preserving the original ordering of the Pauli strings. This procedure guarantees that the Pauli expansion contains at most K terms at any point during the evolution, thereby enforcing a strict and controllable upper bound on the computational cost.

We apply this fixed- K truncation after each imaginary time operator. Since each operation can generate at most twice as many Pauli terms, the intermediate Pauli basis size is bounded by $2K$, ensuring that the overall computational scaling remains tractable throughout the simulation.

To assess the scalability of the algorithm under a fixed computational budget, we perform numerical experiments using the fixed- K truncation scheme while increasing the system size N . We set K equal to the number of Pauli terms generated for $N = 12$ spins in the absence of truncation, namely $K = 2,704,156$. Using this fixed value of K , we simulate imaginary time evolution for system sizes ranging from $N = 12$ to $N = 50$ spins in steps of two. The Trotter step size is chosen as $\Delta t = 0.04$, consistent with the previous experiments, and the evolution is carried out up to a maximum imaginary time $t = 20.0$. The results are shown in Fig. 3.

From these simulations, we observe that a fixed- K truncation yields reasonably accurate ground-state energies up to system sizes of approximately $N \simeq 20$. For

larger systems, the ITPP energy saturates and no longer decreases appreciably with increasing N , indicating a breakdown of the approximation due to the imposed constraint on the Pauli basis size. Interestingly, this loss of accuracy coincides with the regime $K < 2^N$, suggesting that the number of Pauli terms required to faithfully approximate the ground-state energy under imaginary time evolution may scale exponentially with system size. By contrast, in the intermediate regime $2^N < K < 4^N$, ITPP maintains low relative error while retaining a number of Pauli terms that is substantially smaller than that of the full Pauli basis.

We emphasize that these observations should be interpreted with caution. Since the truncation parameter K is fixed to a single value determined from the $N = 12$ system, the present results do not allow for a definitive characterization of the asymptotic scaling of the algorithm. Nevertheless, the fixed- K experiments provide valuable insight into the practical limitations of ITPP and clearly illustrate the challenges of maintaining an accurate approximation under a fixed computational budget.

As an additional consistency check, we performed simulations in which the truncation size was scaled exponentially with the system size for moderate system sizes, setting $K = 2^N$ for N ranging from 12 to 24 in steps of two. In this regime, both the absolute and relative errors remained approximately constant as the system size increased. Although these results are limited to a restricted range of system sizes, they provide further support for the interpretation that the loss of accuracy observed under fixed- K truncation is primarily due to insufficient operator support during imaginary time evolution. More generally, these observations are consistent with the possibility that maintaining a comparable level of accuracy may require a number of Pauli terms that grows rapidly, potentially exponentially, with system size.

IV. CONCLUSIONS

In this work, we extend the Pauli Propagation framework to imaginary-time evolution. By deriving explicit update rules governing the propagation of Pauli operators under imaginary time operators generated by Pauli strings, we introduced an operator-based algorithm for approximating imaginary time evolution. This extension enables the direct computation of thermal and ground-state properties via imaginary time dynamics, while preserving the key computational advantages of Pauli Propagation, including the efficient bitstring representation of Pauli operators and the use of simple algebraic update rules.

At a formal level, we demonstrated that Pauli Propagation can be consistently generalized to imaginary time evolution. In the absence of truncation, the resulting imaginary time Pauli Propagation algorithm (ITPP) exactly reproduces Trotterized imaginary time evolution, thereby providing an alternative operator-based formulation of imaginary time dynamics. We benchmarked ITPP on the one-dimensional transverse-field Ising model in the ordered phase, employing both coefficient-based and fixed-rank truncation strategies to control the growth of the Pauli basis.

When truncation is introduced, ITPP yields approximate ground-state energies with controllable accuracy while retaining only a fraction of the full Pauli expansion. In particular, coefficient-threshold truncation enables a systematic trade-off between accuracy and computational cost, allowing meaningful ground-state energy estimates to be obtained with significantly fewer Pauli terms than required by the full, non-truncated evolution.

At the same time, our numerical results highlight important limitations of Pauli-based imaginary time evolution. For coefficient-threshold truncation, the number of Pauli terms required to maintain a given level of accuracy grows rapidly with system size, while fixed number truncation experiments further show that, under a constant computational budget, ITPP accurately captures ground-state energies only up to moderate system sizes, beyond which the approximation deteriorates. Additional consistency checks, in which the truncation size was scaled exponentially with system size for small systems, suggest that maintaining comparable accuracy may require an exponentially growing number of Pauli terms. While these observations do not constitute a definitive characterization of the asymptotic scaling, they clearly illustrate the challenges associated with controlling operator growth in imaginary time Pauli Propagation while maintaining accurate ground-state energy approximations.

Beyond closed-system dynamics, the extension to

imaginary time evolution also suggests a natural pathway toward simulating open quantum system dynamics when combined with Pauli Propagation for real-time evolution. In principle, this can be achieved by working with the vectorized Lindblad equation, in which the evolution of the vectorized density matrix is generated by an operator containing both Hermitian (unitary) and anti-Hermitian (non-unitary) contributions. Within this framework, the unitary part can be treated using real-time Pauli Propagation, while the non-unitary part can be handled using the imaginary time extension introduced here. Related strategies have been explored for simulating open quantum dynamics on quantum hardware in Ref. [14]. However, implementing this approach within the present framework would require a reformulation of Pauli Propagation in terms of vectorized operators rather than operator-valued observables, necessitating substantial modifications to the current software infrastructure. A vectorized Pauli-based approach has been investigated in Ref. [10], and a detailed exploration of this direction is left for future work.

Taken together, our results establish ITPP as a useful and flexible tool for exploring imaginary time dynamics and ground-state properties in small to intermediate system sizes, while also clarifying the fundamental challenges posed by operator growth in non-unitary evolution. By making these limitations explicit, this work provides a clear baseline for future developments aimed at mitigating operator proliferation through improved truncation schemes or enhanced Pauli-based ansätze, as well as for extending Pauli Propagation to the simulation of open quantum system dynamics.

V. ACKNOWLEDGMENTS

RGL thanks Shao-Hen Chiew for valuable discussions and feedbacks. This work was supported by the project PID2023-152724NA-I00, with funding from MCIU/AEI/10.13039/501100011033 and FSE+, the Severo Ochoa Grant CEX2023-001292-S, Generalitat Valenciana grant CIPROM/2022/66, the Ministry of Economic Affairs and Digital Transformation of the Spanish Government through the QUANTUM ENIA project call - QUANTUM SPAIN project, and by the European Union through the Recovery, Transformation and Resilience Plan - NextGenerationEU within the framework of the Digital Spain 2026 Agenda, and by the CSIC Interdisciplinary Thematic Platform (PTI+) on Quantum Technologies (PTI-QTEP+). This project has also received funding from the European Union's Horizon 2020 research and innovation program under grant agreement CaLIGOLA MSCA-2021-SE-01-101086123. RGL is funded by grant CIACIF/2021/136 from Generalitat Valenciana.

[1] U. Schollwöck, Annals of Physics **326**, 96–192 (2011).

[2] R. Orús, Annals of Physics **349**, 117–158 (2014).

[3] W. M. C. Foulkes, L. Mitas, R. J. Needs, and G. Rajagopal, Rev. Mod. Phys. **73**, 33 (2001).

[4] F. F. Assaad and H. G. Evertz, World-line and Determinantal Quantum Monte Carlo Methods for Spins, Phonons and Electrons, in *Computational Many-Particle Physics*, edited by H. Fehske, R. Schneider, and A. Weiße (Springer Berlin Heidelberg, Berlin, Heidelberg, 2008) pp. 277–356.

[5] J. Eisert, M. Cramer, and M. B. Plenio, Rev. Mod. Phys. **82**, 277 (2010).

[6] P. Calabrese and J. Cardy, Journal of Statistical Mechanics: Theory and Experiment **2005**, P04010 (2005).

[7] E. Y. Loh, J. E. Gubernatis, R. T. Scalettar, S. R. White, D. J. Scalapino, and R. L. Sugar, Phys. Rev. B **41**, 9301 (1990).

[8] M. Troyer and U.-J. Wiese, Phys. Rev. Lett. **94**, 170201 (2005).

[9] P. Rall, D. Liang, J. Cook, and W. Kretschmer, Phys. Rev. A **99**, 062337 (2019).

[10] M. S. Rudolph, E. Fontana, Z. Holmes, and L. Cincio, Classical surrogate simulation of quantum systems with lowesa (2023), arXiv:2308.09109 [quant-ph].

[11] T. Begušić, J. Gray, and G. K.-L. Chan, Science Advances **10**, 10.1126/sciadv.adk4321 (2024).

[12] T. Begušić and G. K.-L. Chan, PRX Quantum **6**, 020302 (2025).

[13] A. Angrisani, A. Schmidhuber, M. S. Rudolph, M. Cerezo, Z. Holmes, and H.-Y. Huang, Phys. Rev. Lett. **135**, 170602 (2025).

[14] H. Kamakari, S.-N. Sun, M. Motta, and A. J. Minnich, PRX Quantum **3**, 010320 (2022).

[15] M. Motta, C. Sun, A. T. K. Tan, M. J. O'Rourke, E. Ye, A. J. Minnich, F. G. S. L. Brandão, and G. K.-L. Chan, Nature Physics **16**, 205–210 (2019).

[16] S. McArdle, T. Jones, S. Endo, Y. Li, S. C. Benjamin, and X. Yuan, npj Quantum Information **5**, 10.1038/s41534-019-0187-2 (2019).

[17] A. Anglés-Castillo, L. Ion, T. Pandit, R. Gomez-Lurbe, R. Martínez, and M. A. Garcia-March, Understanding quantum imaginary time evolution and its variational form (2025), arXiv:2510.02015 [quant-ph].

[18] G. B. Mbeng, A. Russomanno, and G. E. Santoro, SciPost Physics Lecture Notes 10.21468/scipostphyslectnotes.82 (2024).

[19] M. S. Rudolph, T. Jones, Y. Teng, A. Angrisani, and Z. Holmes, arXiv preprint arXiv:2501.13101 (2025).

Appendix A: Pauli Propagation Rules for imaginary time Evolution

In this appendix, we derive the propagation rules governing the imaginary time evolution of a Pauli string P generated by another Pauli string Q . We consider the non-unitary imaginary time evolution operator

$$V_Q(\tau) = e^{-\frac{\tau}{2}Q}, \quad (\text{A1})$$

where $\tau \in \mathbb{R}$ denotes the imaginary time and Q is a Pauli string satisfying $Q^2 = \mathbb{I}$. The imaginary time-evolved Pauli operator is defined as

$$P(\tau) = V_Q^\dagger(\tau) P V_Q(\tau). \quad (\text{A2})$$

Using the expansion

$$V_Q(\tau) = \cosh\left(\frac{\tau}{2}\right) \mathbb{I} - \sinh\left(\frac{\tau}{2}\right) Q, \quad (\text{A3})$$

and substituting it into Eq. (A2), we obtain the general expression

$$V_Q^\dagger(\tau) P V_Q(\tau) = \cosh^2\left(\frac{\tau}{2}\right) P - \cosh\left(\frac{\tau}{2}\right) \sinh\left(\frac{\tau}{2}\right) (QP + PQ) + \sinh^2\left(\frac{\tau}{2}\right) QPQ. \quad (\text{A4})$$

Since P and Q are Pauli strings, they either commute or anticommute, leading to two distinct cases.

$$\text{Anticommuting case } \{P, Q\} = 0.$$

If P and Q anticommute, the second term in Eq. (A4) vanishes because $QP + PQ = 0$. Using $QPQ = -P$, we find

$$V_Q^\dagger(\tau) P V_Q(\tau) = \left[\cosh^2\left(\frac{\tau}{2}\right) - \sinh^2\left(\frac{\tau}{2}\right) \right] P = P, \quad (\text{A5})$$

where we have used the identity $\cosh^2(x) - \sinh^2(x) = 1$.

Commuting case $[P, Q] = 0$

If P and Q commute, $QP = PQ$, and Eq. (A4) simplifies to

$$V_Q^\dagger(\tau) P V_Q(\tau) = \left[\cosh^2\left(\frac{\tau}{2}\right) + \sinh^2\left(\frac{\tau}{2}\right) \right] P - 2 \cosh\left(\frac{\tau}{2}\right) \sinh\left(\frac{\tau}{2}\right) QP. \quad (\text{A6})$$

Using the identities $\cosh^2(x) + \sinh^2(x) = \cosh(2x)$ and $2 \cosh(x) \sinh(x) = \sinh(2x)$, this expression can be written as

$$V_Q^\dagger(\tau) P V_Q(\tau) = \cosh(\tau) P - \sinh(\tau) QP. \quad (\text{A7})$$

Summary

The propagation of a Pauli string P under imaginary time evolution generated by a Pauli string Q is therefore given by

$$V_Q^\dagger(\tau) P V_Q(\tau) = \begin{cases} P, & \{P, Q\} = 0, \\ \cosh(\tau) P - \sinh(\tau) QP, & [P, Q] = 0. \end{cases} \quad (\text{A8})$$

These propagation rules form the basis of Pauli propagation under imaginary time evolution employed in imaginary time Pauli propagation (ITPP).